Mycologia Iranica 11(2): 19 –31, 2024 **Original Article** DOI:10.22043/MI.2024.367640.1293

Green synthesis of nano-sized calcite crystals by ureolytic *Acremonium egyptiacum* associated with grapevine decline

B. Rezaeian
Department of Biological Science, Faculty of Science, University of Kurdistan, Sanandaj, Kurdistan, Iran

M. Ashengroph ✉
Department of Biological Science, Faculty of Science, University of Kurdistan, Sanandaj, Kurdistan, Iran
Research Center for Nanotechnology, University of Kurdistan, Sanandaj, Kurdistan, Iran

J. Abdollahzadeh ✉
Department of Plant Protection, Agriculture Faculty, University of Kurdistan, Sanandaj, Kurdistan, Iran

M. Moetasam Zorab
Department of Physics, College of Science, University of Halabja, Kurdistan region, Iraq

S. Piri Kakihai
Department of Plant Protection, Agriculture Faculty, University of Kurdistan, Sanandaj, Kurdistan, Iran

Abstract: Nano-calcite, or calcium carbonate nanoparticles, is valued for its stability and versatile applications, particularly in agriculture, where it enhances soil quality, regulates pH, improves nutrient delivery, and promotes sustainable crop yields. In this research, nano-calcite was synthesized using *Acremonium egyptiacum* IRAN 5247C, isolated from grapevine necrotic wood, under sedimentary conditions through fungal urease production. Key factors including urea and calcium concentrations, pH, incubation time, and temperature were optimized using a one-factor-at-a-time (OFAT) approach, resulting in a maximum yield of 595 mg of calcite per 10 ml of solution. Field emission scanning electron microscopy (FE-SEM) imaging revealed that the nanocrystals were predominantly spherical, averaging 73.5 ± 8.02 nm in size, with a distribution range of 25 to 125 nm. X-ray diffraction (XRD) and Fourier transform infrared-Raman (FTIR-Raman) spectroscopy confirmed a well-defined crystalline calcite structure characterized by carbonate ions. This study reports the first synthesis of nano-calcite using *Acremonium egyptiacum*, with precise control over particle shape and size, an ideal feature for applications in concrete reinforcement, bio-cementation, and agriculture.

Keywords: Fungal bio-cementation, Fungal-mediated nano-calcite, Urease activity.

INTRODUCTION

Microbially induced calcium carbonate precipitation (MICP) is a process where microorganisms, such as fungi, promote the formation of calcium carbonate ($CaCO_3$) through metabolic activities like urea hydrolysis. This process raises pH by releasing hydroxide ions, which stimulates $CaCO_3$ precipitation. MICP has been widely studied for its potential in soil stabilization and other biogeochemical applications (Konstantinou and Wang 2023). Significant attention has been paid to biological nano-sized calcium carbonate, or nano-calcite, because of its cost-effectiveness, minimal toxicity, and environmental benefits. Beyond its biomedical applications (Zhao et al. 2022), it has been applied to environmental engineering to remove pollutants (Boyjoo et al. 2014), agriculture to enhance crop yields by improving soil quality (Kumara et al. 2019), and construction to strengthen concrete and cement (Sharma and Ashish 2023). Various methods can be used to synthesize nano-sized calcium carbonate, including mechanical methods, emulsions, precipitation, carbonation, and polymer-mediated techniques (Fadia et al. 2021). These methods are energy- and resource-intensive, generating significant chemical waste and are environmentally massive worthless processes. Nano-sized calcium carbonate synthesis using fungi and bacteria is an environmentally more sustainable and safe approach. Bio-synthesized $CaCO_3$ nanoparticles are noted for their cost-effectiveness, minimal toxicity, biological and cytological compatibility, pH sensitivity, gradual biodegradability, and ecological comity (Motlhalamme et al. 2023). This approach makes nano-calcite production more cost-effective and environmentally friendly by minimizing harsh chemicals and energy consumption. Numerous

Submitted 10 Nov. 2024, accepted for publication 16 Dec. 2024
✉ Corresponding Authors: E-mail: m.ashengroph@uok.ac.ir, j.abdollahzadeh@uok.ac.ir

https://mij.areeo.ac.ir

species from the bacterial genera *Lysinibacillus* (Shirakawa et al. 2011), *Sporosarcina* (Konstantinou and Biscontin 2022), *Virgibacillus* (Silva-Castro et al. 2015), *Bacillus* (Salehi et al. 2022), *Pseudomonas* (Guo et al. 2021, Ghorbanzadeh et al. 2021), and *Staphylococcus* (Karatas et al. 2008), as well as various fungal genera including *Myrothecium*, *Fusarium*, *Aspergillus*, *Trichoderma*, *Pestalotiopsis*, *Neurospora*, *Chrysosporium*, *Mortierella*, and *Cephalotrichum* (Li et al. 2015, Van Wylick et al. 2021), have been found which can biosynthesize calcium carbonate nanoparticles and microparticles. These organisms have facilitated the precipitation of calcium carbonate through complex biochemical processes involving enzymatic actions and interactions with the environment. Additionally, cyanobacteria (e.g. *Synechocystis pevalekii*) (Sidhu et al. 2022), and some archaea (Görgen et al. 2021) also play significant roles in calcium carbonate biosynthesis. Fungi frequently outperform bacteria in nanoparticle synthesis, owing to their unique ability to modify chemical environments and produce specialized enzymes. Their active production of capping and reducing agents is a notable advantage, distinguishing fungi as highly efficient nanoparticle synthesizers. They are also capable of bio-fabricating large quantities of uniformly sized and shaped nanoparticles extracellularly, with high enzyme activity for bio-reduction (Loshchinina et al. 2022). Thus, employing fungi for nano-calcite synthesis is a promising and eco-friendly strategy in future studies. Calcite precipitation efficiency is influenced by various environmental factors including temperature, salinity, calcium chloride, and urea. These factors affect the calcium compound's solubility and the rate of biochemical reactions. Additionally, calcite precipitation is affected by pH levels and the presence

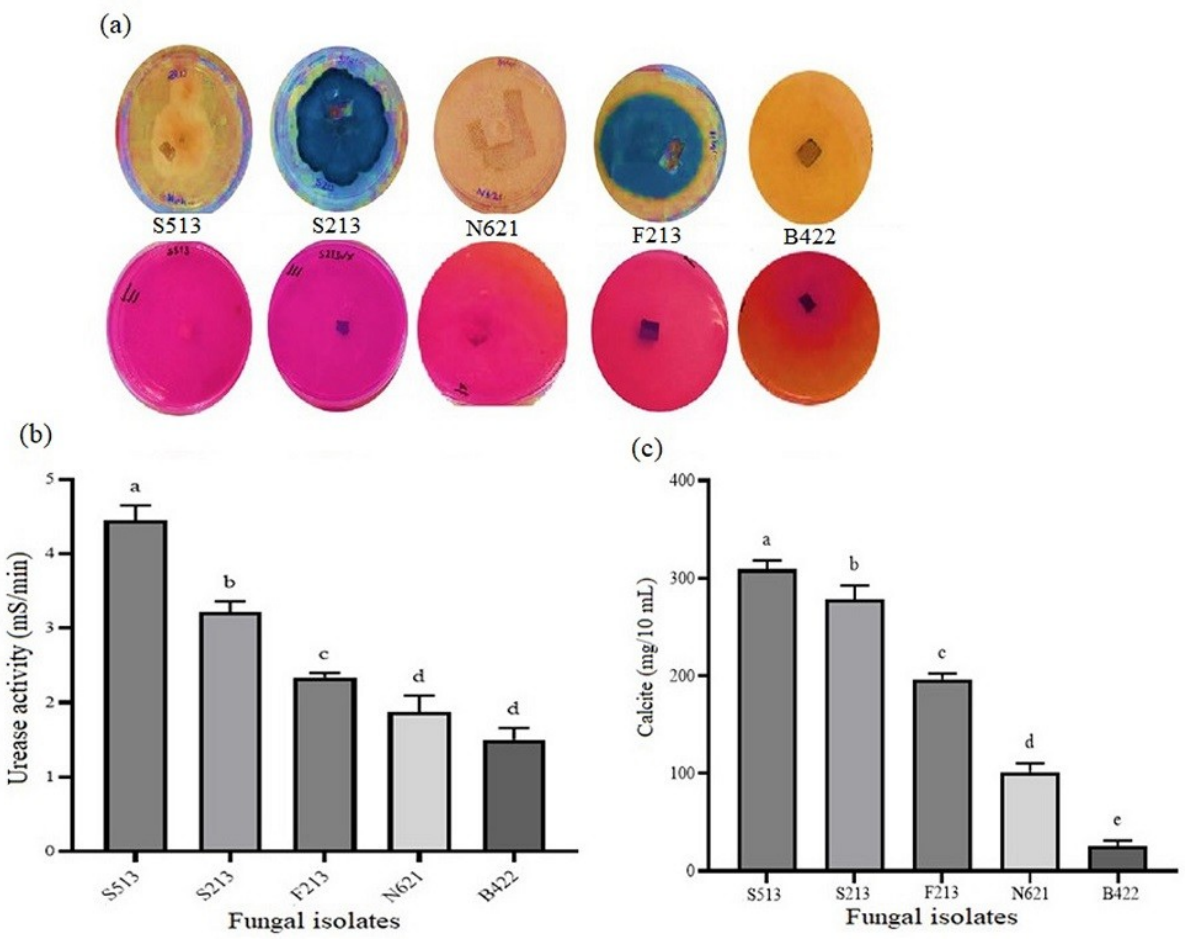

Fig. 1. Urease activity and calcium carbonate precipitation in fungal isolates. a. Urease activity in fungal isolates on 2% urea agar after 48 h at 25°C; b. Conductometric comparison of urease activity, with each milliSiemens per minute corresponding to the hydrolysis of 11 mM urea per minute; c. Calcium carbonate precipitation in fungal isolates using a reaction mixture with 1 M urea and calcium chloride at 25°C and pH 6. Statistical differences are indicated by different lowercase letters ($P < 0.05$).

of other ions or organic compounds (Kim et al. 2018, Wang et al. 2023). Understanding these factors is crucial for optimizing calcite production and enhancing its applications in fields such as environmental remediation and materials science. Recently we have focused on the potential of fungi for biosynthesis of nano-sized calcium carbonate particles. This study evaluates the capacity of *Acremonium egyptiacum* IRAN 5247C, isolated from declined grapevine twigs and trunks, to produce nano-calcite under varying experimental conditions. To the best of our knowledge, no previous research has specifically investigated *A. egyptiacum* for calcite production. These findings open up promising opportunities for the potential application of fungal species in bioremediation, biomaterials development, and sustainable agriculture.

MATERIALS AND METHODS

Fungal isolates

This study investigated calcite biosynthesis using five fungal strains including IRAN 5247C (= S513), B422, F213, N621, and S213. These isolates were obtained from necrotic woody tissues of grapevine twigs and trunks collected from Kouzaran, Kermanshah Province, and provided by the Mycology Laboratory at the Faculty of Agriculture, University of Kurdistan. The fungal isolates were purified using single-spore and hyphal tip techniques on potato dextrose agar (PDA).

Qualitative assessment of urease activity

To assess quality of urease activity of the fungal strains, 5-mm discs from 14-day-old colonies grown on PDA were transferred on Christensen's urea agar (0.1% peptic digest of animal tissue, 0.1% dextrose, 0.5% sodium chloride, 0.12% disodium phosphate, 0.08% monopotassium phosphate, 0.0012% phenol red, and 1.5% agar) supplemented with 2% urea sterilized using Millipore membrane filters with 0.22

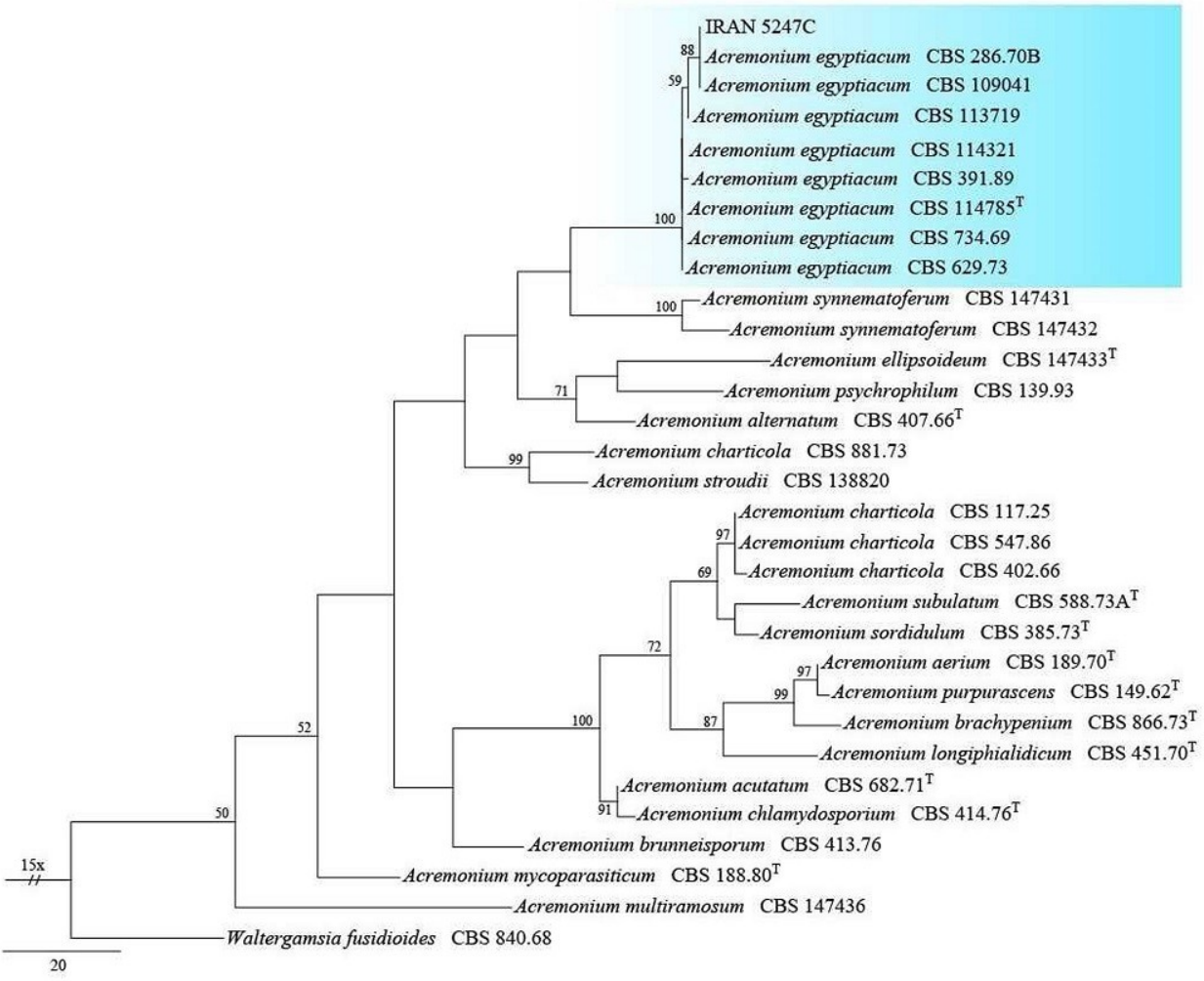

Fig. 2. One of the 23 most parsimonious trees generated based on ITS sequence data for *Acremonium* species. Maximum parsimony bootstrap values >50% are given at the nodes. The tree was rooted with *Waltergamsia fusidioides* CBS 840.68. Scale bar = 20 nucleotide changes. ^{T} indicates ex-type strain.

µm pores and incubated for 48 h at 25 °C. Urease activity was detected by urea hydrolysis, resulting in ammonia production and increased alkalinity (Omoregie et al. 2019) which leads to a change in the phenol red indicator from yellow to pink or red. A negative control was prepared using sterile-supplemented Christensen's urea agar with no fungal colony.

Fungal extract preparation and urease activity quantification

Fungal isolates were cultured in 250 ml Erlenmeyer flasks containing urea-modified AP1 (Agar Plate 1) medium consisting of 40 mM urea, 4 mM dipotassium hydrogen phosphate ($K_2HPO_4 \cdot 3H_2O$), 0.8 mM magnesium sulfate heptahydrate ($MgSO_4 \cdot 7H_2O$), 0.2 mM calcium chloride dihydrate ($CaCl_2 \cdot 2H_2O$), 1.7 mM sodium chloride (NaCl), 0.009 mM ferric chloride hexahydrate ($FeCl_3 \cdot 6H_2O$), 0.014 mM zinc sulfate heptahydrate ($ZnSO_4 \cdot 7H_2O$), 0.018 mM manganese sulfate monohydrate ($MnSO_4 \cdot H_2O$), and 0.016 mM copper sulfate pentahydrate ($CuSO_4 \cdot 5H_2O$). After 7 days of incubation on the rotary shaker at 200 rpm and 25°C under dark conditions, the mycelial biomass was collected through centrifugation at 4000 × g for 30 min and passed through a 0.45 µm membrane filter. The mycelial mass was washed three times with sterile deionized water and incubated in sterile deionized water for an additional 7 days before being utilized in the synthesis of calcium carbonate (Ashengroph and Rabiei 2023). The urease activity of the fungal strains was quantitatively measured using the electrical conductivity method. One ml of the fungal extract was added to 9 ml of urea solution 1.1 M prepared in sterile distilled water. Electrical conductivity changes were recorded using a conductivity meter at five intervals over 5-minute. The slope of the resulting graph was used to determine urease activity, with a steeper slope indicating higher activity. Urease activity was expressed in millisiemens per minute (mS/min), where each mS/min corresponded to the hydrolysis of 11 mM of urea per min (Harkes et al. 2010).

Assessment and optimization of calcite precipitation

Calcite production was assessed by mixing the fungal extracts with a reactive solution containing nickel chloride as a urea cofactor, along with urea and calcium chloride. The mixture was incubated at 25°C for 24 h, after which the sediment was collected, washed, dried at 60°C, and weighed to assess calcite yield (Krajewska 2017, Gandali Mostafa et al. 2024). Optimization experiments were conducted using assessment of urea and calcium chloride concentration, pH, and incubation time effects on calcite production. These factors were systematically varied across different experiments, with incubation periods ranging from 12 to 60 h. Analysis of variance (ANOVA) and Tukey's test at a 95% confidence level were employed to determine the optimal conditions for efficient calcite synthesis.

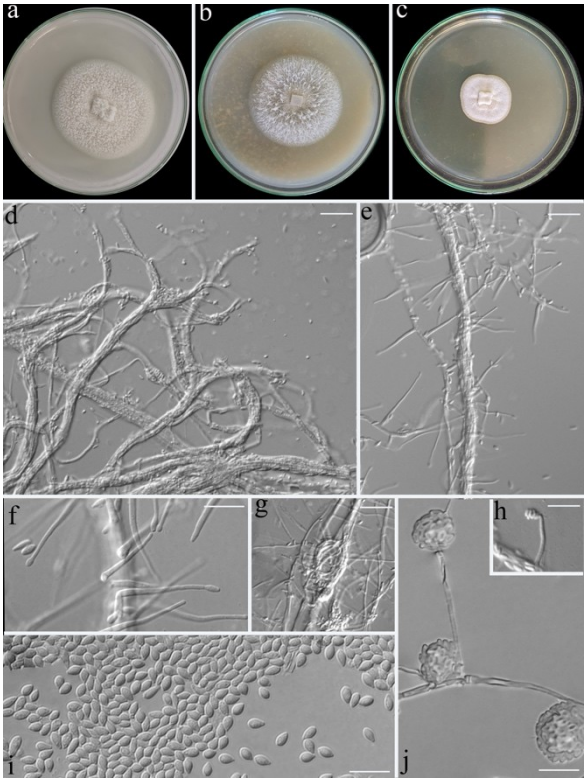

Fig. 3. Morphology of *Acremonium egyptiacum* IRAN 5247C. a. Colony on PDA; b. Colony on OA; c. Colony on MEA; d. Mycelial ropes; e, f. Phialides; g. Mycelial coil; h, j. Conidial heads; i. Conidia. Scale bars: d, e, g, h = 20 µm; f, i, j = 10 µm.

Characterization of fungal isolate IRAN 5247C

Total genomic DNA was extracted from 7-day colony grown on PDA at 25°C following the modified method of Raeder and Broda (1985) as described by Abdollahzadeh et al. (2009). Nuclear ribosomal internal transcribed spacer (ITS) region, consisting ITS1-5.8S-ITS2 rDNA, as a universal DNA barcode for fungi was amplified using the universal primers ITS5 (5'-TCCGTAGGTGAACCTGCGG-3') and ITS4 (5'-TCCTCCGCTTATTGATATGC-3') (White 1990). The PCR conditions were: 95°C for 3 min, followed by 35 cycles of 95°C for 60 s, 52°C for 60 s, 72°C for 90 s, and a final extension of 72°C for 5 min. PCR products were purified and sequenced by BGI (China) via BMG (Bio Magic Gene) Co. (Alborz, Iran). The sequences were extracted using BioEdit Sequence Alignment Editor v.7.0.9.0 software and deposited in

GenBank. The generated sequence of ITS region together with the sequences of type or authentic strains of congeneric species based on BLAST search of NCBI was subjected to phylogenetic analysis using the maximum parsimony (MP) method as described by Abdollahzadeh et al. (2014). Phylograms were viewed with FigTree v. 1.4.3 (http://tree.bio.ed.ac.uk/software/figtree) and edited in Adobe Illustrator CS2 v. 12.0.0. For morphological identification, colony morphology studied on PDA in 90 mm petri plates at 25 °C after 14 days. Microscopic features were observed and documented with an Olympus BX51 microscope equipped with an Olympus DP72 camera.

Characterization of nano-calcite

The calcite nanocrystals produced by isolate IRAN 5247C were first washed with 96% ethanol and sterile deionized water, and then freeze-dried. Subsequent analysis was conducted using field emission scanning electron microscopy (FESEM, TSCAN, MIRA3) equipped with Energy-Dispersive X-ray spectroscopy (EDX) to determine particle structure and size distribution. Histograms and average particle sizes were generated using ANIX Emica software. EDX provided elemental composition data, while Fourier-transform infrared spectroscopy (FTIR, BRUKER) was utilized to assess structural properties within 500-1400 cm^{-1} range. Additionally, X-ray diffraction (XRD, Philips PW1730) analysis with CuKα radiation was performed to set out (or describe) the crystal structure and phase characteristics over an angular range of 5 to 80 degrees.

RESULTS AND DISCUSSION

Screening fungal isolates for urea activity and calcite precipitation

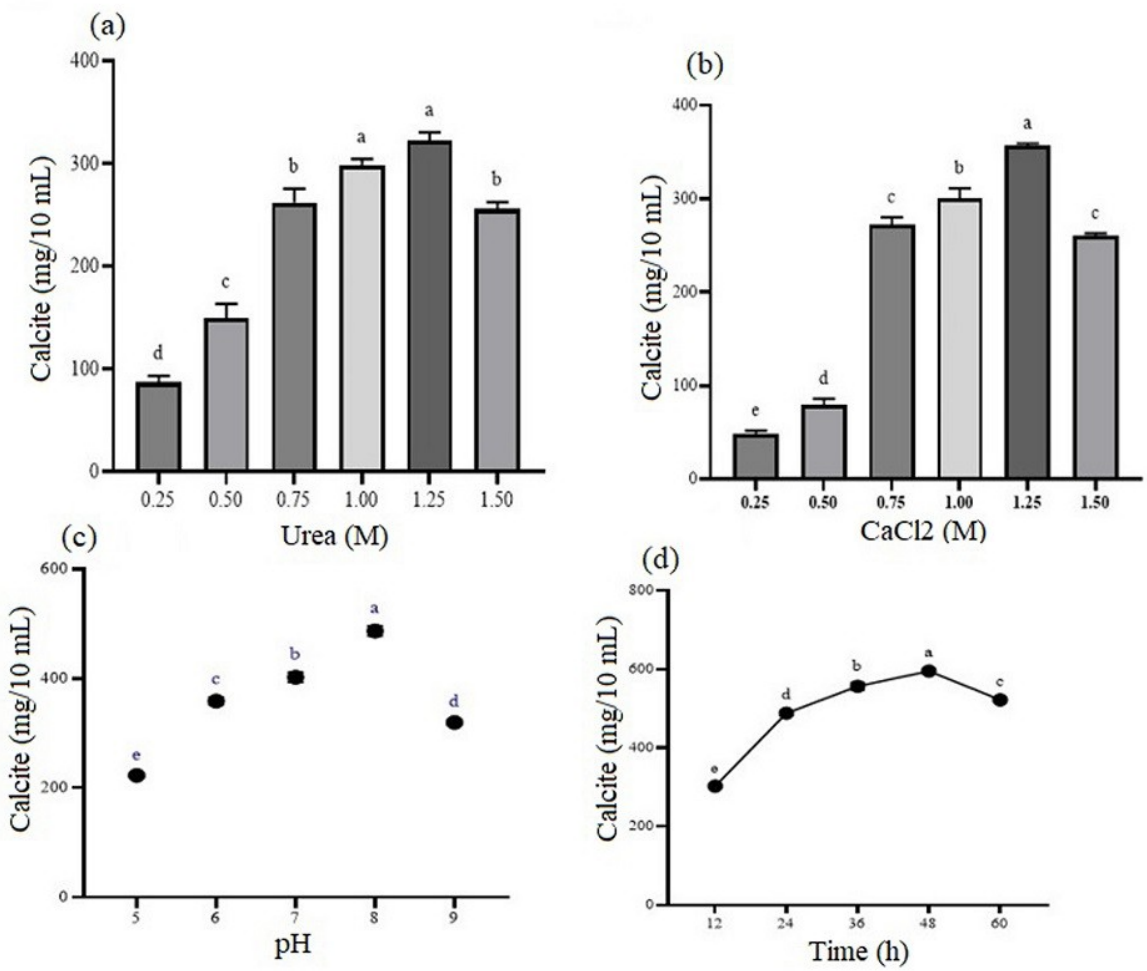

Fig. 4. Comparison of calcium carbonate precipitation at different: a. urea concentrations; b. calcium chloride concentrations; c. pH levels; d. incubation times. Statistical differences are indicated by different lowercase letters ($P < 0.05$).

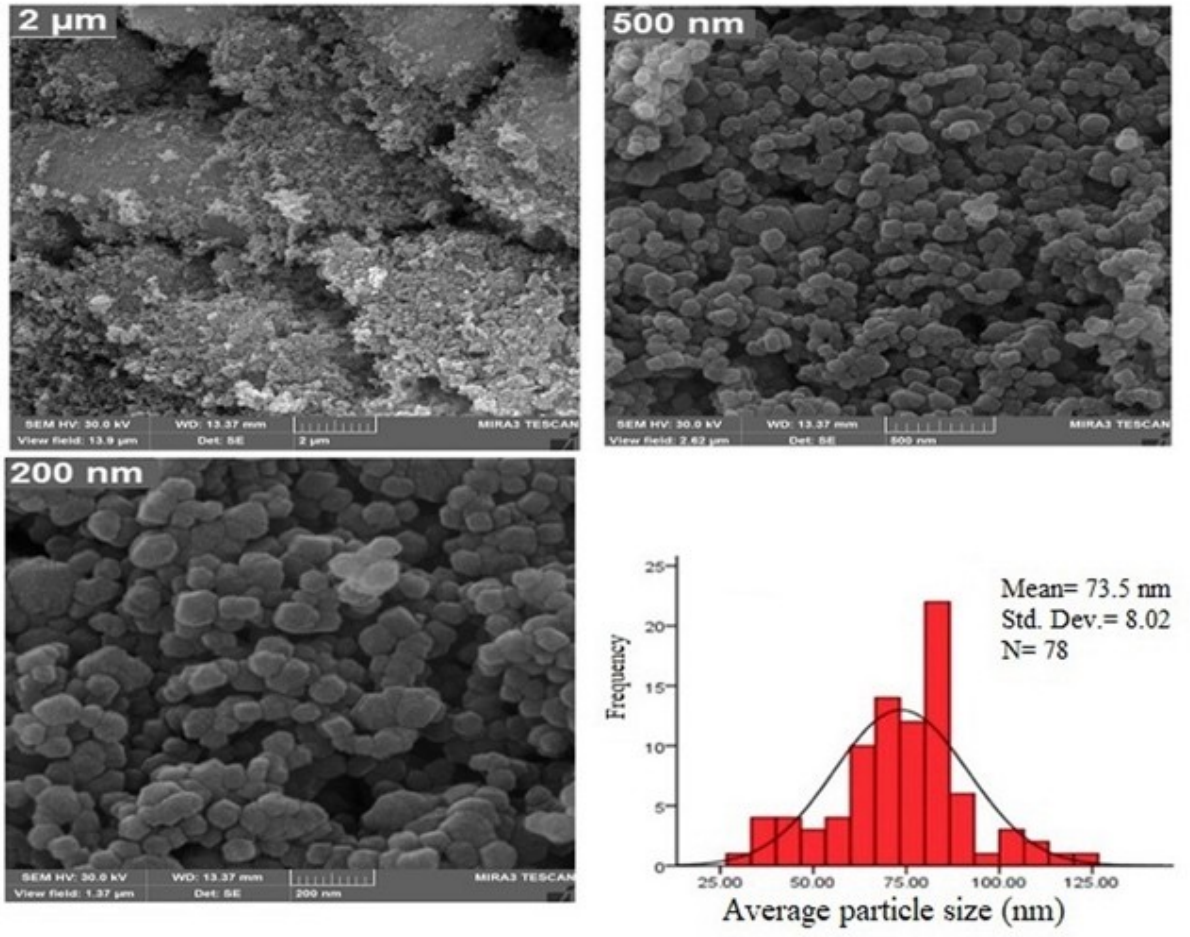

Fig. 5. Field Emission Scanning Electron Microscopy (FESEM) analysis of calcite nanoparticles synthesized by the fungal extract of *Acremonium egyptiacum* IRAN 5247C under optimal experimental conditions.

In a preliminary test, eighteen fungal isolates were screened for urea hydrolytic efficiency on Christensen's urea agar plates. After 48-h incubation, five isolates (IRAN 5247C = S513, S213, N621, F213, and B422) demonstrated significant urease activity, indicated by a distinct bright pink or red color change (Fig. 1a). Urease activity causes ammonia production, shifting the pH and altering the medium's color from yellow to pink. Strain IRAN 5247C exhibits the most significant color change, indicating the highest urease activity and likely the highest calcite production. Urease activity was quantified using a conductometric method with a 1.1 M urea solution. Each fungal extract (1 mL) was mixed with 9 ml of urea solution at 25 °C for 5 min. The resulting increase in electrical conductivity was measured and expressed in milliSiemens per min (mS/min) (Fig. 1b). Isolate IRAN 5247C exhibited the highest urease activity, corroborating the color change results. Calcite precipitation was assessed by measuring the amount of calcite produced per 10 ml of the reaction mixture. Fungal extracts were combined with a 1 M calcium chloride solution, revealing significant differences in calcite production among the examined strains. Isolate IRAN 5247C produced 309 mg of calcite per 10 mL, significantly higher than the other isolates with average calcite production as follows: S213 (264 mg), F213 (196 mg), N621 (101 mg), and B422 (25 mg) (Fig. 1c).

Characterization of isolate IRAN 5247C

BLAST search of NCBI with generated ITS sequence of isolate IRAN 5247C gave the closesthit to *Acremonium egyptiacum*. Phylogenetic analysis placed isolate IRAN 5247C (PQ358698) together with type strain (CBS 114785) of *A. egyptiacum* in a well-supported clade (Fig. 2). Colony morphology and microscopic features of our isolate are shown in Fig. 3. Species of *Acremonium* are cosmopolitan and found mainly as soil-borne saprophytes or as pathogens of plants, fungi, animals or humans (Pérez□Cantero and Guarro 2020, Kim et al. 2021). These fungi are of significant importance in agriculture, forestry, food storage, industry, clinical

mycology, and pharmaceuticals (Hou et al. 2023). *Acremonium* species are especially noted for their capacity to produce a wide range of novel and bioactive secondary metabolites, with over 350 such compounds identified to date (Tian et al. 2017). These metabolites with antimicrobial activity and enzyme inhibition properties resulted in significant potential of *Acremonium* species in medicine, agriculture, and industry (Qin et al. 2024). In this study, *A. egyptiacum* is specifically recognized for its production of urease, an enzyme critical for the biogenic formation of calcium carbonate. This enzymatic activity is particularly valuable for application in soil stabilization and waste management.

Process parameters for maximum calcite precipitation

As deduced from the literature, precise control of key parameters is essential for optimizing calcite production, particularly in biotechnological applications such as bio-cementation, soil stabilization, and environmental remediation (Fadia et al. 2021, Ojha et al. 2021, Erdmann and Strieth 2023). In this study, four primary factors urea and calcium chloride concentration, pH, and incubation time were found which affected calcite synthesis by *A. egyptiacum* IRAN 5247C (Fig. 4a-d). As shown in Fig. 4a, calcite production increased with rising urea concentrations from 0.25 M to 1.25 M, peaking at 1.25 M (~322 mg/10 ml). A slight decrease at 1.50 M (~255 mg/10 ml) suggests that extra high urea concentrations may inhibit calcite production, likely due to osmotic stress or toxicity to fungal cells. Urea is essential for providing carbonate ions necessary for calcite formation. Statistical analysis revealed no significant difference between 1.0 M and 1.25 M, indicating that 1.0 M urea is effective for maximizing calcite production. Therefore, 1.0 M was determined as the optimal concentration, balancing carbonate ion availability and fungal metabolic activity while avoiding inhibitory effects at higher concentrations. Moreover, calcite production is significantly influenced by calcium chloride concentration. As illustrated in Fig. 4b, calcite production peaked at 1.25 M (~356 mg/10 ml) and declined at 1.50 M (~260 mg/10 ml). Calcium ions are crucial for calcite formation, and production peak at 1.25 M obviously suggests optimal concentration to maximize production. However, extra-high calcium chloride concentrations may cause ionic imbalances or toxicity, leading to reduced calcite synthesis. Consistent with studies on *Sporosarcina pasteurii*, urea concentration was similarly crucial for calcite precipitation in this study. However, the optimal calcium chloride concentration in this study (1.25 M) is higher than those reported for bacteria, likely reflecting the distinct metabolic requirements of fungal strains compared to bacteria (Rautela and Rawat 2020).

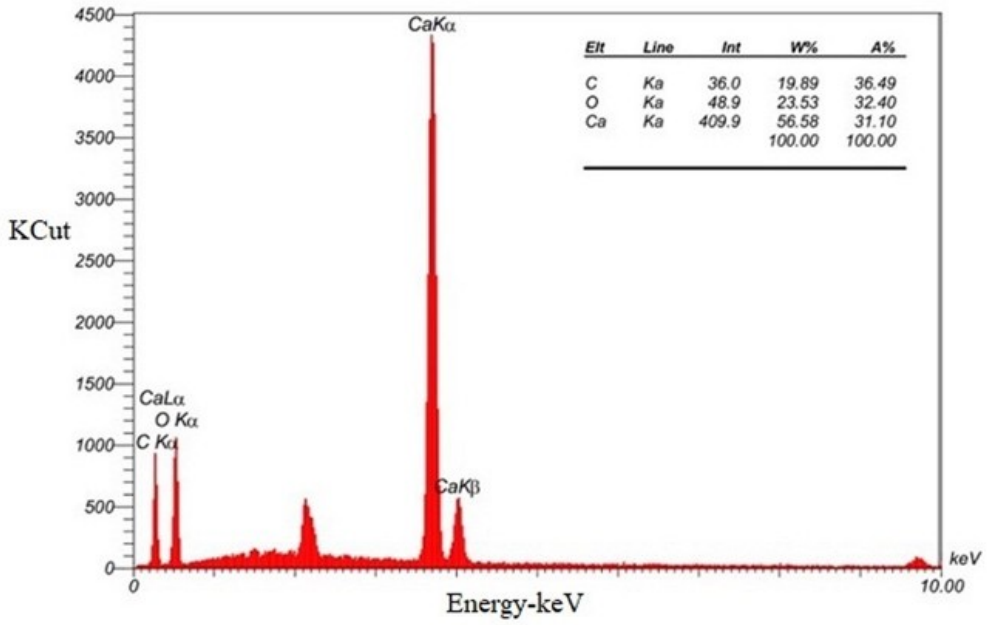

Fig. 6. Energy-Dispersive X-ray Spectroscopy (EDX) analysis of calcite nanoparticles synthesized by the fungal extract of *Acremonium egyptiacum* IRAN 5247C under optimal experimental conditions.

As shown in Fig. 4c, calcite synthesis varies significantly depending on pH, as the highest yield was observed at pH 8 (~486 mg/10 ml) and lower calcite yields at both lower pH (pH 5, 6) and higher pH (pH 9) levels. The reaction environment pH significantly impacts the solubility and availability of carbonate ions, as well as the metabolic activity of the fungal strain. The peak achieved at pH 8 suggests the optimal pH for calcite precipitation under tested conditions. At lower pH levels, carbonate ion availability may be restricted, while higher pH levels likely reduce calcium solubility, resulting in less efficient calcite formation. The optimal pH 8 determined in this study, is comparable to optimal pH 7 for calcite production using bacteria (Kim et al. 2018) and probably indicates that microbial calcite precipitation generally favors a neutral to slightly alkaline pH range. The amount of calcite production increased over time, reaching its maximum (~595 mg/10 ml) at 48 hours. However, it slightly decreased to around ~522 mg/10 ml at 60 hours (Fig. 4d). In this study, the optimal incubation time for calcite synthesis was determined to be 48 hours, after which production declined. This differs from bacterial systems, where calcite precipitation typically occurs over a span of 3 days (Kim et al., 2018). The faster peak observed in the fungal process highlights its potential as a more efficient bioprocess under the tested conditions. Our findings indicated that optimizing parameters such as urea and calcium chloride concentration, pH, and incubation time are crucial for maximizing calcite production. To improve the overall efficiency of the bioprocess, further studies are necessary to figure out the reasons for yield decline at higher concentrations and longer incubation times.

Characterization of calcium carbonate nanocrystals

FESEM analysis revealed that the majority of nanoparticles exhibited a spherical or near-spherical morphology, with an average size of 73.5 ± 8.02 nm and a size distribution ranging from 25 to 125 nm (Fig. 5). This narrow size range is remarkable comparing to the broader size distributions with less control over uniformity in *Klebsiella pneumoniae* (Render et al. 2016) and *S. pasteurii* (Kim et al. 2018). The precise control of

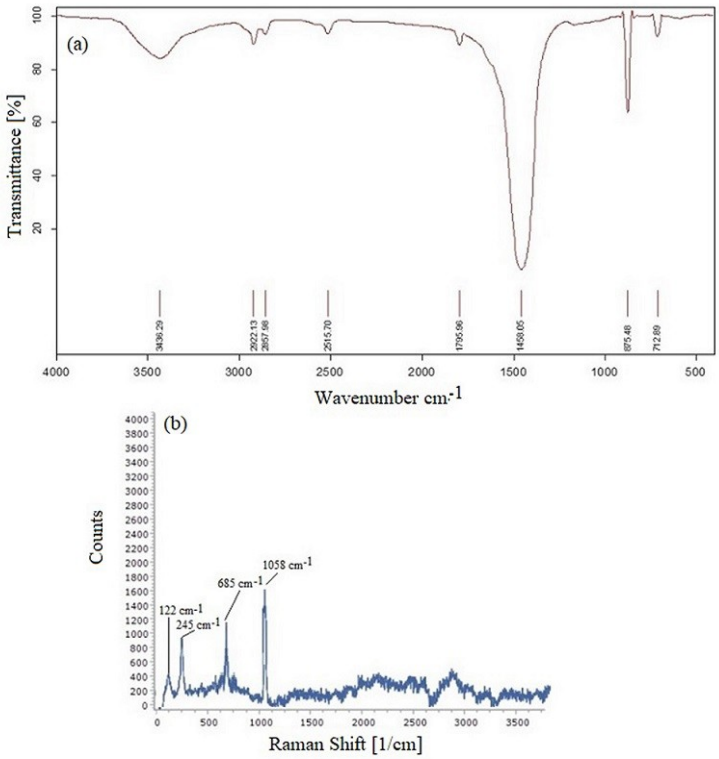

Fig. 7. a. Fourier-transform infrared spectroscopy (FTIR) analysis; b. Raman spectra of calcite nanoparticles synthesized by the fungal extract of *Acremonium egyptiacum* IRAN 5247C under optimal conditions.

particle size in this study makes it valuable for applications requiring consistency, such as drug delivery and bio-cementation. The smooth surface morphology observed through FESEM further improves the functional properties of nano-calcite as suitable features for industrial and biotechnological applications including stability, bioactivity, and ability to effectively interact with other materials. EDX analysis confirmed the elemental composition of calcium, carbon, and oxygen, indicating a crystalline calcite structure (Fig. 6). FTIR analysis (Fig. 7a) confirmed the formation of calcite by detecting the characteristic vibrational modes of carbonate ions. Peaks at 1458 cm^{-1}, 712 cm^{-1}, and 875 cm^{-1} corresponded to the symmetric stretching and bending vibrations of the carbonate group. Additionally, a broad peak at 3436 cm^{-1} indicated the presence of hydroxyl groups, suggesting water or amino compounds on the nano-calcite surface. The FTIR results confirm the successful formation of calcite and provide insights into the surface chemistry of the nano-calcite, influencing its interaction with other materials in industrial applications (Cai et al. 2010). As FTIR complement, Raman spectrum (Fig. 7b) revealed distinct structural characteristics of the synthesized nano-calcite. The prominent peak at 1085 cm^{-1} is associated with the symmetric stretching vibrations of the carbonate group (CO_3^{2-}), a hallmark of the calcite structure. Additionally, a peak at 685 cm^{-1} corresponds to the bending vibrations of the carbonate group, while smaller peaks at 245 cm^{-1} and 122 cm^{-1} are related to the lattice vibrations of calcite, further confirming the composition and crystalline structure of the nano-calcite (Donnelly et al. 2017). The combined FTIR and Raman spectra confirm a well-defined calcite structure, with carbonate group (CO_3^{2-}) which is a key functional factor. The presence of distinct peaks associated with carbonate groups strongly validates the successful synthesis of nano-calcite, characterized by a strong crystalline structure. XRD analysis (Fig. 8) identified distinct peaks at 23.02°, 29.38°, 35.94°, 43.13°, 47.09°, 48.49°, and 57.36°, corresponding to the (012), (104), (110), (202), (016), (018), and (122) calcite planes. These peaks aligned with standard reference patterns, confirming the crystalline nature and high purity of the synthesized nano-calcite, essential for material applications (Fadia et al. 2021, Render et al. 2016). The high purity, smooth morphology, and precise particle size control of the nano-calcite produced by *A. egyptiacum* IRAN 5247C confirmed its potential for eco-friendly and sustainable production, offering a greener alternative to conventional methods. Our findings show a promising future for applied mycology to exploit fungi in bio-cementation, environmental remediation and advanced biomaterial development. The narrow particle size range achieved here, which is rarely found in the literature, significantly highlights the innovation of

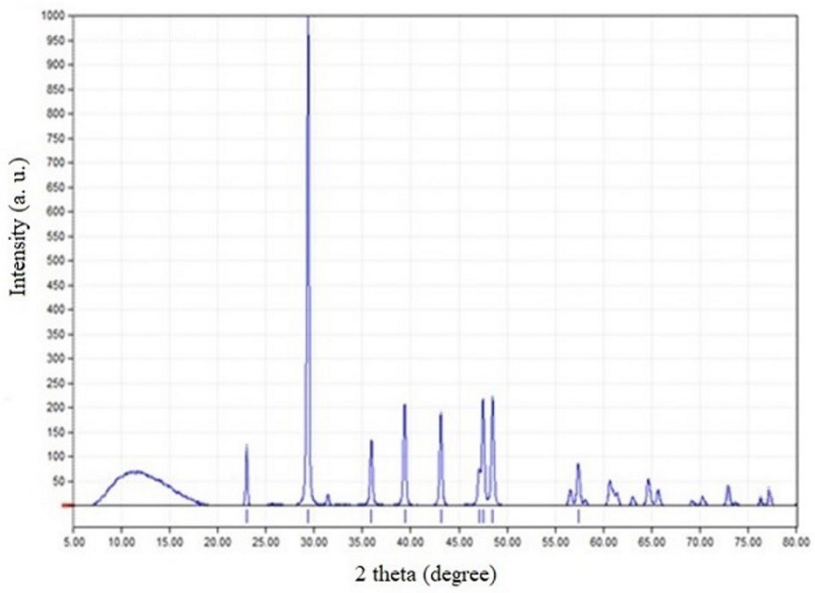

Fig. 8. X-ray Diffraction (XRD) analysis of calcite nanoparticles synthesized by the fungal extract of *Acremonium egyptiacum* IRAN 5247C under optimal conditions.

our study. Future researches could explore alternative metabolic pathways, such as organic acid consumption, to improve particle size and morphology.

CONCLUSION

In this study, isolate IRAN 5247C a novel ureolytic fungus obtained from declined grapevine twigs and trunks, which morphologically and phylogenetically identified as *Acremonium egyptiacum*, showed a significant potential for eco-friendly synthesis of calcium carbonate (nano-calcite) nanocrystals. Among eighteen fungal isolates, IRAN 5247C with the highest urease activity and calcite production is introduced as a potent candidate for various biotechnological applications. Optimization of key parameters urea and calcium chloride concentrations, pH, and incubation time resulted here in significant calcite precipitation, often with nanocrystal size from 65.5 to 81.5 nm. Nano-calcite produced by *Acremonium egyptiacum* IRAN 5247C exhibits ideal features such as narrow size distribution, spherical morphology, and high chemical stability for applications in concrete reinforcement, crack repair, bio-cementation, medical fields, and agriculture. Nano-calcite properties improve soil fertility, nutrient delivery, sustainable agriculture, and environmental remediation. Future studies should examine different metabolic pathways, especially those involving organic acids, to improve the control over calcium carbonate nanoparticle size and shape, which could result in more efficient and eco-friendly production techniques.

ACKNOWLEDGMENTS

This work was financially supported by the Research Council of the University of Kurdistan under grant agreement number 00/9/34027/2021.

REFERENCES

Abdollahzadeh, J., Goltapeh, E.M., Javadi, A., Shams-Bakhsh, M., Zare, R. and Phillips, A.J.L. 2009. *Barriopsis iraniana* and *Phaeobotryon cupressi*: two new species of the *Botryosphaeriaceae* from trees in Iran. Persoonia 23(1): 1–8.

Abdollahzadeh, J., Hosseini, F. and Javadi, A., 2014. New records from *Botryosphaeriaceae* (Ascomycota) for mycobiota of Iran. Mycologia Iranica 1(1): 43–51.

Ashengroph, M. and Rabiei, Z. 2023. Green copper carbonate nanoparticles produced by the ureolytic fungus *Alternaria* sp. strain ccf7 and their antibacterial activity. Jentashapir Journal of Cellular and Molecular Biology 14(2): e136448.

Boyjoo, Y., Pareek, V.K. and Liu, J. 2014. Synthesis of micro and nano-sized calcium carbonate particles and their applications. Journal of Materials Chemistry A 2: 14270–14288.

Cai, G.B., Chen, S.F., Liu, L., Jiang, J., Bin, Yao, H., Xu, A.W. and Yu, S.H. 2010. 1,3-Diamino-2-hydroxypropane-*N*,*N*,*N*′,*N*′-tetraacetic acid stabilized amorphous calcium carbonate: nucleation, transformation and crystal growth. CrystEngComm 12: 234–241.

Donnelly, F.C., Purcell-Milton, F., Framont, V., Cleary, O., Dunne, P.W. and Gun'ko, Y.K. 2017. Synthesis of $CaCO_3$ nano- and micro-particles by dry ice carbonation**.** Chemical Communications 53: 6657–6660.

Erdmann, N. and Strieth, D. 2023. Influencing factors on ureolytic microbiologically induced calcium carbonate precipitation for bio-cementation. World Journal of Microbiology and Biotechnology 39: 61.

Fadia, P., Tyagi, S., Bhagat, S., Nair, A., Panchal, P., Dave, H., Dang, S. and Singh S. 2021. Calcium carbonate nano- and microparticles: synthesis methods and biological applications. 3 Biotech 11: 457.

Gandali Mostafa, N., Ghezelbash, G. and Shafiei, M. 2024. Investigating the different amounts of urea and calcium on the formation of different forms of calcium carbonate in precipitation medium using *Sporosarcina pasteurii*. Cellular and Molecular Research 37(1): 30–44.

Ghorbanzadeh, N., Shokati, R., Farhangi, M.B., Shabanpour, M. and Unc, A. 2021. Effect of the biogenic precipitation of calcium carbonate on bacterial transport in sand columns. Ecohydrology & Hydrobiology 21(2): 280–291.

Görgen, S., Benzerara, K., Skouri-Panet, F., Gugger, M., Chauvat, F. and Cassier-Chauvat, C. 2021. The diversity of molecular mechanisms of carbonate biomineralization by bacteria. Discover Materials 1: 2.

Guo, N., Wang, Y., Hui, X., Zhao, Q., Zeng, Z., Pan, S., Guo, Z., Yin, Y. and Liu, T. 2021. Marine bacteria inhibit corrosion of steel via synergistic biomineralization. Journal of Materials Science and Technology 66: 82–90.

Harkes, M.P., Van Paassen, L.A., Booster, J.L., Whiffin, V.S. and van Loosdrecht, M.C. 2010. Fixation and distribution of bacterial activity in sand to induce carbonate precipitation for ground reinforcement**.** Ecological engineering 36: 112–117.

Hou, L.W., Giraldo, A., Groenewald, J.Z., Rämä, T., Summerbell, R.C., Huang, G.Z., Cai, L. and Crous, P.W. 2023. Redisposition of acremonium-like fungi in *Hypocreales*. Studies in Mycology 105: 23–203.

Karatas, I., Kavazanjian, J.E. and Rittmann, B.E. 2008. Microbially induced precipitation of calcite using *Pseudomonas denitrificans*. In: Proceedings of 1st bio-geo engineering conference, TU Delft and Deltares, Delft, The Netherlands. pp. 58–66.

Kim, G., Kim, J. and Youn, H. 2018. Effect of temperature, pH, and reaction duration on microbially induced calcite precipitation. Applied Sciences 8(8): 1277.

Kim, H.J., Li, X.J., Kim, D.C., Kim, T.K., Sohn, J.H., Kwon, H., Lee, D., Yim, J.H. and Oh, H. 2021. PTP1B inhibitory secondary metabolites from an antarctic fungal strain *Acremonium* sp. SF-7394. Molecules 26: 5505.

Konstantinou, C. and Biscontin, G. 2022. Experimental investigation of the effects of porosity, hydraulic conductivity, strength, and flow rate on fluid flow in weakly cemented bio-treated sands. Hydrology 9(11): 190.

Konstantinou, C. and Wang, Y. 2023. Unlocking the potential of microbially induced calcium carbonate precipitation (MICP) for hydrological applications: A review of opportunities, challenges, and environmental considerations. Hydrology 10(9): 178.

Krajewska, B. 2017. Urease-aided calcium carbonate mineralization for engineering applications: A review. Journal of Advanced Research 13: 59–67.

Kumara, K., Wathugala, D. and Hafeel, R.F. 2019. Effect of nano calcite foliar fertilizer on the growth and yield of rice (*Oryza sativa*). Journal of Agricultural Sciences – Sri Lanka. 14: 154.

Li, Q., Csetenyi, L., Paton, G.I. and Gadd, G.M. 2015. $CaCO_3$ and $SrCO_3$ bioprecipitation by fungi isolated from calcareous soil. Environmental Microbiology 17(8): 3082–3097.

Loshchinina, E.A., Vetchinkina, E.P. and Kupryashina, M.A. 2022. Diversity of biogenic nanoparticles obtained by the fungi-mediated synthesis: A review. Biomimetics (Basel) 8(1): 1.

Motlhalamme, T., Mohamed, H., Kaningini, A.G., More, G.K., Thema, F.T. and Maaza, M. 2023. Bio-synthesized calcium carbonate ($CaCO_3$) nanoparticles: Their anti-fungal properties and application as nanofertilizer on *Lycopersicon esculentum* growth and gas exchange measurements. Plant Nano Biology 6: 100050.

Ojha, N., Aich, P. and Das, N. 2021. Process optimization of microbially induced calcite precipitation by ureolytic yeast *Spathospora* sp. NN04 using Box-Behnken design: A novel approach towards bio-cementation**.** Journal of Applied Biotechnology Reports 8(3): 303–311.

Omoregie, A.I., Ong, D.E.L. and Nissom, P.M. 2019. Assessing ureolytic bacteria with calcifying abilities isolated from limestone caves for biocalcification. Letters in Applied Microbiology 68: 173–181.

Pérez-Cantero, A. and Guarro, J. 2020. *Sarocladium* and *Acremonium* infections: New faces of an old opportunistic fungus. Mycoses 63(11): 1203–1214.

Qin, Y., Lu, H., Qi, X., Lin, M., Gao, C., Liu, Y. and Luo, X. 2024. Recent advances in chemistry and bioactivities of secondary metabolites from the genus *Acremonium*. Journal of Fungi 10(1): 37.

Raeder, U. and Broda, P. 1985. Rapid preparation of DNA from filamentous fungi. Applied Microbiology 1: 17–20.

Rautela, R. and Rawat, S. 2020. Analysis and optimization of process parameters for in vitro biomineralization of $CaCO_3$ by Klebsiella pneumoniae, isolated from a stalactite from the Sahastradhara cave. RSC Advances 10(14): 8470–8479.

Render, D., Samuel, T., King, H., Vig, M., Jeelani, S., Babu, R.J. and Rangari, V. 2016. Biomaterial-derived calcium carbonate nanoparticles for enteric drug delivery. Journal of Nanomaterials 2016: 3170248.

Salehi, P., Dabbagh, H. and Ashengroph, M. 2022. Effects of microbial strains on the mechanical and durability properties of lightweight concrete reinforced with polypropylene fiber. Construction and Building Materials 322: 126519.

Sharma, H. and Ashish, D.K. 2023. Nano $CaCO_3$ for enhancing properties of cement-based materials: A comprehensive review. Journal of Sustainable Cement-Based Materials 12(12): 1475–494.

Shirakawa, M.A., Cincotto, M.A., Atencio, D., Gaylarde, C.C. and John, V.M. 2011. Effect of culture medium on biocalcification by *Pseudomonas putida, Lysinibacillus Sphaericus* and *Bacillus subtilis.* Brazilian Journal of Microbiology 42(2): 499-507.

Sidhu, N., Goyal, S. and Reddy, M.S. 2022. Biomineralization of cyanobacteria *Synechocystis pevalekii* improves the durability properties of cement mortar. AMB Express 12(1): 59.

Silva-Castro, G.A., Uad, I., Gonzalez-Martinez, A., Rivadeneyra, A., Gonzalez-Lopez, J. and Rivadeneyra, M.A. 2015. Bioprecipitation of calcium carbonate crystals by bacteria isolated from saline environments grown in culture media amended with seawater and real brine. BioMed Research International 2015: 816102.

Tian, J., Lai, D. and Zhou, L. 2017. Secondary metabolites from *Acremonium* fungi: Diverse structures and bioactivities. Mini-Reviews in Medicinal Chemistry 17(7): 603–632.

Van Wylick, A., Monclaro, A.V., Elsacker, E., Vandelook, S., Rahier, H., De Laet, L., Cannella, D. and Peeters, E. 2021. A review on the potential of filamentous fungi for microbial self-healing of concrete. Fungal Biology and Biotechnology 8(1): 16.

Wang, Y., Konstantinou, C., Tang, S. Chen, H. 2023. Applications of microbial-induced carbonate precipitation: A state-of-the-art review. Biogeotechnics 1: 100008.

White, T. J., Bruns, T., Lee, S., Taylor, J. 1990. Amplification and direct sequencing of fungal ribosomal RNA genes for phylogenetics. In: Innis, M. A,, Gelfand, D. H., Sninsky, J. J., White, T. J. (eds). PCR protocols: a guide to methods and applications: 315–322. Academic Press, San Diego, California.

Zhao, P., Tian, Y., You, J., Hu, X. and Liu, Y. 2022. Recent advances of calcium carbonate nanoparticles for biomedical applications. Bioengineering 9: 691.

سنتز سبز کریستال‌های نانوکلسیت توسط قارچ اورئولیتیک *Acremonium egyptiacum* مرتبط با زوال انگور

بنت الهدی رضائیان[۱]، مراحم آشنگرف[۱و۲]✉، جعفر عبداله زاده[۳]✉، موسی معتصم زوراب[۴]، سودابه پیری کاکیهایی[۳]

۱- گروه علوم زیستی، دانشکده علوم، دانشگاه کردستان، سنندج، ایران

۲- مرکز پژوهشی نانو، دانشگاه کردستان، سنندج، ایران

۳- گروه گیاهپزشکی، دانشکده کشاورزی، دانشگاه کردستان، سنندج، ایران

۴- گروه فیزیک، دانشکده علوم، دانشگاه حلبچه، اقلیم کردستان، عراق

چکیده: نانوکلسیت یا نانوذرات کربنات کلسیم به دلیل پایداری بالا و کاربردهای متنوع خود، به‌ویـژه در کشـاورزی، کـه در بهبـود کیفیت خاک، تنظیم pH، افزایش انتقال مواد مغذی و ارتقاء عملکرد پایدار محصولات مؤثر است، از اهمیت ویژه‌ای برخوردار است. در این پژوهش، نانوکلسیت توسط *Acremonium egyptiacum* IRAN 5247C، جدا شده از بافت های چوبی نکروتیک تنه و شاخه انگور، در شرایط رسوبی از طریق تولید اوره‌آز قارچی سـنتز شـد. عوامـل کلیـدی ماننـد غلظت اوره و کلسـیم، pH، زمان و دمای انکوباسیون با روش تک‌فاکتوری (OFAT) بهینه‌سازی شدند که منجر به حداکثر بازده ۵۹۵ میلی‌گرم کلسیت در هر ۱۰ میلی‌لیـتر محلول گردید. تصاویر FE-SEM نشان داد که نانوکریستال‌ها عمدتاً کروی هستند و اندازه متوسـط آن‌هـا ۸/۰۲ ± ۷۳/۵ نـانومتر با محدوده توزیع ۲۵ تا ۱۲۵ نانومتر است. آنالیزهای XRD و طیف‌سنجی FTIR-Raman ساختار کریستالی کلسیت با حضور یون‌های کربنات را تأیید کردند. این مطالعه، نخستین بار سنتز نانوکلسیت با استفاده از *A. egyptiacum* را گزارش می‌کنـد کـه با کنـترل دقیق بر شکل و اندازه ذرات، ویژگی‌هایی ایده‌آل برای کاربرد در تقویت بتن، سمنتاسیون زیستی و کشاورزی ارائه می‌دهد.

کلمات کلیدی: سیمان زیستی قارچی، فعالیت اوره‌آز، نانوکلسیت قارچی

مکاتبه کننده: مراحم آشنگرف و جعفر عبداله زاده Email: m.ashengroph@uok.ac.ir, j.abdollahzadeh@uok.ac.ir

تاریخ دریافت: ۱۴۰۳/۰۸/۲۰ تاریخ پذیرش: ۱۴۰۳/۰۹/۲۶